Published in final edited form as:
Biol Reprod. 2001 July ; 65(1): 318–332.

Spermatogenesis in *Bclw*-Deficient Mice[1]

Lonnie D. Russell[2,4], **Jeff Warren**[4], **Luciano Debeljuk**[4], **Laura L. Richardson**[3,5], **Patryce L. Mahar**[6], **Katrina G. Waymire**[6], **Scott P. Amy**[6], **Andrea J. Ross**[6,7], and **Grant R. MacGregor**[2,6]

[4] Department of Physiology, Southern Illinois University School of Medicine, Carbondale, Illinois 62901-6512

[5] Department of Biochemistry and Cellular and Molecular Biology, University of Tennessee, Knoxville, Tennessee 37996

[6] Center for Molecular Medicine, Emory University School of Medicine, Atlanta, Georgia 30322

[7] Graduate Program in Biochemistry, Cell and Developmental Biology, Emory University, Atlanta, Georgia 30322

Abstract

Bclw is a death-protecting member of the Bcl2 family of apoptosis-regulating proteins. Mice that are mutant for *Bclw* display progressive and nearly complete testicular degeneration. We performed a morphometric evaluation of testicular histopathology in *Bclw*-deficient male mice between 9 days postnatal (p9) through 1 yr of age. Germ cell loss began by p22, with only few germ cells remaining beyond 7 mo of age. A complete block to elongated spermatid development at step 13 occurred during the first wave of spermatogenesis, whereas other types of germ cells were lost sporadically. Depletion of Sertoli cells commenced between p20 and p23 and continued until 1 yr of age, when few, if any, Sertoli cells remained. Mitochondria appeared to be swollen and the cytoplasm dense by electron microscopy, but degenerating Bclw-deficient Sertoli cells failed to display classical features of apoptosis, such as chromatin condensation and nuclear fragmentation. Macrophages entered seminiferous tubules and formed foreign-body giant cells that engulfed and phagocytosed the degenerated Sertoli cells. Leydig cell hyperplasia was evident between 3 and 5 mo of age. However, beginning at 7 mo of age, Leydig cells underwent apoptosis, with dead cells being phagocytosed by macrophages. The aforementioned cell losses culminated in a testis-containing vasculature, inter-tubular phagocytic cells, and peritubular cell “ghosts.” An RNA in situ hybridization study indicates that *Bclw* is expressed in Sertoli cells in the adult mouse testis. Consequently, the diploid germ cell death may be an indirect effect of defective Sertoli cell function. Western analysis was used to confirm that Bclw is not expressed in spermatids; thus, loss of this cell type most likely results from defective Sertoli cell function. Because *Bclw* does not appear to be expressed in Leydig cells, loss of Leydig cells in Bclw-deficient mice may result from depletion of Sertoli cells. Bclw-deficient mice serve as a unique model to study homeostasis of cell populations in the testis.

[1]Supported by grants from the NIH (HD36437 to G.R.M. and HD35494 to L.D.R.). Part of this work was performed in the laboratory of M.A. Handel with support from HD31376.

[2]Correspondence: Lonnie D. Russell, Dept. of Physiology, Southern Illinois University, Life Sci II, Room 174, Lincoln Drive, Carbondale, IL 62901-6501. FAX: 618 453 1517; lrussell@siumed.edu, Grant R. MacGregor, Center for Molecular Medicine, Emory University School of Medicine, 1462 Clifton Rd. NE, 403-E, Atlanta, GA 30322. FAX: 404 727 8367; gmacgre@emory.edu.
[3]Current address: Dept. of Anatomy and Cell Biology, Marshall University, Huntington, WV 25704.

Keywords

aging; apoptosis; developmental biology; gametogenesis; Leydig cells; Sertoli cells; testes

INTRODUCTION

Mammalian spermatogenesis occurs in the testis, where germ cell development is intimately supported by Sertoli cells, the somatic component of the seminiferous epithelium. Sertoli cells are responsible for effecting the downstream process of male sexual differentiation [1]. During mouse development, Sertoli cells can be found in the developing gonad by Embryonic Day 11.5 [1]. Sertoli cells are mitotic during embryogenesis, with the exception of a brief period during organization of the testicular cords. In postnatal mice, Sertoli cells complete exit from mitosis by Postnatal Day 17 (p17), concomitant with development of the initial wave of spermatogenesis [2,3]. Exit from mitosis precedes terminal differentiation of Sertoli cells, which includes development of specialized junctional complexes on the lateral sides of the cell that are involved in forming the Sertoli cell barrier [4]. Postmitotic Sertoli cells are not replaced during adult life, and little is currently known about the factors required for survival of postmitotic Sertoli cells in vivo.

Insertional mutagenesis in the mouse is a powerful method for identifying genes that are required for a developmental or homeostatic process. We previously used retro-viral gene trapping to identify a requirement for *Bclw* in mouse spermatogenesis [5]. *Bclw* is a member of the *Bcl2* gene family, which is involved in regulation of apoptosis during development and homeostasis in metazoans. At a simplistic level, the Bcl2 family of proteins is composed of two classes of members: those that help to protect from cell death (e.g., A1, Bcl2, Bclw, $BclX_L$, and Mcl1), and those that help to promote cell death (e.g., Bad, Bak, Bax, Bid, Bik, Bim, Bok, $BclX_S$, Blk, and Hrk). Current models for the function of these two classes of proteins are intricate but, at the fundamental level, involve regulation of the release of cytochrome c from mitochondria [6]. The death-promoting members of the Bcl2 family function to mediate release of cytochrome c, which is a cofactor for adaptor molecules that, in turn, regulate activation of latent enzymes named caspases. The activated caspases digest key proteins within the cell, which ultimately results in the apoptotic death of the cell. Death-protecting members of the Bcl2 family can block the release of cytochrome c by the death-promoting Bcl2 family members, at least in part by physically associating with the death-promoting members [6–9].

Our initial report of Bclw-deficient mice involved characterization of the mutant allele, identification of the testicular cells in which *Bclw* is expressed, and a preliminary description of development of the mutant phenotype in adult animals [5]. In the present study, we have used additional techniques to re-examine the pattern of *Bclw* expression in the adult mouse testis. We provide evidence that *Bclw* is expressed in Sertoli cells, but not in haploid spermatids. We have also extended the previous findings by performing a rigorous quantitative analysis of the developmental course of testicular degeneration in Bclw-deficient mice to more than 1 yr of age, including analysis of the ultrastructural features associated with loss of Bclw-deficient Sertoli cells. We show that the Bclw-deficient mouse has a unique phenotype, in which Sertoli cell loss occurs gradually during a period of 1 yr. Bclw-deficient Sertoli cells do not display many of the classical features of apoptosis while degenerating. Sertoli cells are first shed and then phagocytosed by macrophages that enter seminiferous tubules to form highly phagocytic, multinucleate, foreign-body giant cells. Depletion of Leydig cells via apoptosis follows loss of the Sertoli cell population. Sporadic loss of germ cells begins around p19 and is essentially completed by 6 mo of age. Haploid germ cells arrest at step 13 of spermiogenesis and are phagocytosed. Bclw is not expressed

in haploid germ cells, suggesting that their loss is an indirect effect of Sertoli cell dysfunction. The results provide further information regarding possible functions for *Bclw* in male germ cell development, and they offer novel insight into potential roles for Sertoli cells in regulating homeostasis of the adult Leydig cell population.

MATERIALS AND METHODS

Mice

The derivation and molecular characterization of the gene-trap mutation within the *Bclw* gene (*Bcl2l2* locus) in the ROSA41 strain of mouse has been reported elsewhere [5,10]. Analysis of RNA transcripts by reverse transcription-polymerase chain reaction (PCR) and of proteins by Western blot analysis indicates that the mutant allele is null for a Bclw protein product [5].

Animals used in this study were bred at Emory University, genotyped, and held until specific ages, whereupon they were shipped to Southern Illinois University (SIU) at Carbondale. The number of animals used at each time point was four, with the following exceptions: the 9- to 180-day controls and 240-day mutant group had three animals; the 13-day control group had eight animals; the 23-day control group and 210-day mutant group had two animals; the 43-, 90-, and 240-day control groups had six animals; the 180-day mutant group had one animal; and the 270-day mutant group had five animals. All experiments involving mice were conducted using protocols approved by the Institutional Animal Care and Use Committees of SIU and Emory University.

Assay for Genotyping $Bclw^{Gtrosa41}$ Allele

Genotyping was performed by PCR using a three-primer, two-allele assay. The DNA was extracted from 3-mm, tail-tip biopsy specimens of animals between p9 and p12 by overnight incubation at 55°C in 100 μl of a buffer containing 100 mM Tris-HCl (pH 8.0) at 55°C, 50 mM EDTA, 150 mM NaCl, and 0.5% SDS with proteinase K (Roche, Indianapolis, IN) at 100 μg/ml. Following phenol and chloroform extraction, DNA was precipitated by addition of 2.5 volumes of ice-cold, 100% ethanol. Following washing in 70% ethanol and drying, DNA was resuspended in 200 μl of 10 mM Tris-HCl (pH 7.3) and 1 mM EDTA.

Because excessive DNA resulted in poor PCR efficiency, DNA was diluted 10-fold before use in a PCR. One microliter of DNA was used as template in a 30-μl PCR reaction with the following conditions: 10 mM Tris-HCl (pH 9.0) at 25°C, 50 mM KCl, 0.1% Triton X-100, 1.67 mM $MgCl_2$, 500 μM deoxyribonucleotide triphosphates, 500 nM of primer A (see below), 500 nM of primer B, and 250 nM of primer C, with 1.5 U of *Taq* DNA polymerase in storage buffer B (Promega, Madison, WI). The cycling conditions for the PCR were 94°C for 30 sec, 55°C for 30 sec, 72°C for 60 sec, and a final extension of 7 min at 72°C, all performed in an Ericomp Thermocycler (Ericomp, San Diego, CA). The sequences of the primers used were (all indicated 5′-3′):

Primer A: GTGGCCAGCTGCTTATGCTCTGAA

Primer B: CGACGGGATCCGCCATGTCACAGA

Primer C: GATGCGGAGAGCAGCAATTGAGAA

Primer A hybridizes to both PCR templates, whereas primer B recognizes the mutant-allele template and primer C the wild-type template.

Strain Composition of ROSA41 Mice

The ROSA41 mutation was generated in embryonic stem cells derived from a 129S5/SvEvBrd mouse [10]. The animals used in this study were generated by intercross of heterozygous ROSA41 mutants that were N3 (i.e., two backcross generations) for C57BL/6J. Animals between p9 and more than 12 mo of age were used in the present study. No phenotypic differences were observed between wild-type (+/+) and heterozygous mutant (+/−) ROSA41 animals. Consequently, for this study, these two groups were considered as "controls."

Purification of Male Germ Cells by STA-PUT and Isolation of Testes for Prepubertal Study

Male ICR mice were obtained from Harlan Sprague Dawley, Inc. (In-dianapolis, IN). Enriched germ cell fractions were separated by unit gravity sedimentation on a 2%–4% BSA gradient as described elsewhere [11]. Adult (≥8 wk old) mice were used for collection of round spermatids and residual bodies. Purity of the preparations (i.e., percentage of specific cell type) was determined by differential interference contrast microscopy as described elsewhere [12]. The purity of round spermatids used for Western blot analysis was 67%, whereas the purity of the preparation used for Northern blot analysis was 68%. The main contaminant in each case was residual bodies and/or cytoplasts. The purity of the residual body preparations was 98% for Western and 87% for Northern blot analysis. To study the onset of gene expression during prepubertal development, testes were dissected from p7, p12, p17, p22, p27, and adult mice. In addition, testes were isolated from two mutant strains: XX-sex reversed (*XX Sxr*), and *atrichosis* (*at*). The testes of these animals contain no germ cells. The testes were removed, frozen in liquid nitrogen, and stored at −80°C until used for RNA isolation.

Northern Blot Analysis

The RNA was extracted from the cell fractions and testes as described elsewhere [13]. For each sample, 10 μg of total RNA were analyzed by Northern blot using standard techniques [14]. The cDNA probe was labeled to a specific activity of $1–2 \times 10^9$ disintegrations/μg DNA using the Megaprime Random Prime labeling kit (Amersham Pharmacia, Piscataway, NJ). The blot was hybridized overnight at 60°C in 5× SSC (1× SSC: 0.15 M sodium chloride and 0.015 M sodium citrate). After hybridization, the blot was washed briefly in 2× SSC at room temperature, twice in 2× SSC plus 0.5% SDS for 30 min each at 60°C, and twice in 0.5× SSC plus 0.5% SDS for 30 min each at 60°C. The blot was then exposed to x-ray film (Kodak Biomax MS with intensifying screen; Eastman Kodak, Rochester, NY) at −80°C for 5 days.

Western Blot Analysis

Isolated cell fractions were lysed in 1% (v/v) NP-40-Tris-NaCl buffer as described elsewhere [15]. Protein concentration was determined using a Bradford assay (BioRad, Hercules, CA). Twenty micrograms of total protein were electrophoresed through a 14% (w/v) NuPage gel (Novex, San Diego, CA). Following electroblotting to nitrocellulose, the transfer efficiency was determined by staining in 0.1% (w/v) Ponceau S. The affinity-purified, polyclonal rabbit anti-mouse Bclw peptide antibody used has been described previously [5]. In addition to Bclw (21 kDa), this antibody detects a nonspecific protein of approximately 18 kDa. Membranes were blocked overnight, reacted with primary antibody (1:100), washed, and signal detected using a horse radish peroxidase-conjugated secondary antibody (donkey anti-rabbit; Amersham Pharmacia) in conjunction with enhanced chemiluminescence (Amersham Pharmacia).

In Situ Hybridization

Tissues were dissected, washed once in cold phosphate-buffered saline (PBS), and fixed in 4% (w/v) paraformaldehyde (EM Sciences, Fort Washington, PA) in 0.1 M PBS (pH 7.5) for 16 h at 4°C with rocking. Subsequently, tissues were rinsed twice for 15 min each in 15 ml of PBS at 4°C, dehydrated through graded ethanols at room temperature, and cleared twice for 30 min each in Histoclear (National Diagnostics, Atlanta, GA). Infiltration was performed by immersion under 20 mm Hg vacuum using a 1:1 mixture of Paraplast Plus:Histoclear, followed by three changes in Paraplast Plus (Oxford Labware, St. Louis, MO) at 58°C under vacuum for 20 h total. Tissue sections (7 μm) were lifted on poly-lysine-treated slides and incubated overnight on a slide warmer at 37°C.

To prepare digoxigenin (DIG)-labeled riboprobes, a 1537-base pair *Xho*I fragment from the 3′-untranslated region (UTR) of a mouse *Bclw* cDNA (GenBank accession no. AF030769) was cloned into pBS KS-, linearized with an appropriate restriction enzyme, and synthesized using in vitro transcription with a DIG RNA labeling kit (Roche) for 2 h at 37°C according to the manufacturer's instructions. Labeled probes were visualized on an agarose gel and quantified by comparison to a known amount of λ *Hin*dIII DNA fragments.

Hybridization was performed as described elsewhere [16], but with the following modifications: All washes were at room temperature unless otherwise specified. Sections were deparaffinized twice in xylene for 10 min, rehydrated through graded ethanols, and washed twice in reagent-grade H_2O for 5 min each. Sections were immersed in 0.2 M HCl for 20 min to increase accessibility of the riboprobe. After washing in PBS for 5 min, tissue sections were fixed in 4% paraformaldehyde in 0.1 M PBS (pH 7.5) for 20 min. To facilitate more efficient penetration of the riboprobe, tissue sections were treated with 20 μg/ml of proteinase K in 50 mM Tris-HCl and 5 mM EDTA (pH 8.0) for 5 min. After washing in PBS for 5 min, sections were postfixed in 4% paraformaldehyde in 0.1 M PBS (pH 7.5) for 20 min. To minimize nonspecific binding of the probe, tissue sections were washed for 5 min in PBS, then acetylated with a solution containing 0.63 ml of glacial acetic acid in 250 ml of triethanolamine hydrochloride (pH 8.0). Subsequently, sections were washed for 5 min in PBS and dehydrated through graded ethanols. After air drying, sections were prehybridized for a minimum of 2 h at 50°C in a solution of 50% deionized formamide, 3× SSC, 500 μg/ml of yeast RNA, 1× Denhardt solution, 66 mM Na-phosphate buffer (pH 8.0), and 5 mM EDTA. Hybridization was performed overnight for 16 h in a humidified (3× SSC, 50% formamide) chamber at 50°C using a hybridization buffer consisting of prehybridization buffer plus 10% (w/v) dextran sulfate (Amersham Pharmacia) and 1 μg/ml of DIG-labeled riboprobe.

Excess probe was removed by washing twice in solution I (50% form-amide, 5× SSC, 1% SDS) at 60°C for 30 min each. After three washes of 5 min each at room temperature in solution II (0.5 M NaCl, 10 mM Tris-HCl [pH 7.5], 0.1% Tween 20 [v/v]), tissue sections were treated with 20 μg/ml of RNase A (Roche) in solution II for 45 min at 37°C. Subsequently, sections were washed in solution II for 5 min at 37°C, washed twice in solution III (50% formamide, 2× SSC) at 60°C for 30 min each, and then washed twice in PBT (PBS containing 0.1% Tween 20 [v/v]) at room temperature for 20 min each. Nonspecific antibody binding was minimized by preincubating sections in blocking solution (10% sheep serum [v/v] in PBT) for a minimum of 2 h at room temperature. Sections were incubated with an anti-DIG, alkaline phosphatase-conjugated antibody (Roche) diluted 1:1000 in 1% sheep serum (v/v) in PBT for 16 h at 4°C.

Excess antibody was removed by washing in PBT three times for 30 min each at room temperature. Subsequently, sections were washed in NTMT (100 mM Tris-HCl [pH 9.5], 50 mM $MgCl_2$, 100 mM NaCl, 0.1% Tween 20 [v/v], 2 mM levamisole) three times for 5 min

each at room temperature. Sections were overlaid with 150 μl of freshly prepared color solution consisting of 3.5 μl of 5-bromo-4-chloro-3-indolyl phosphate (50 mg/ml stock in dimethylformamide) and 4.5 μl of nitroblue tetrazolium salt (75 mg/ml stock in 70% dimethylformamide) and incubated in a humidified container in the dark at 37°C for up to 48 h until the desired signal intensity was achieved. The color reaction was stopped by washing in PBT, the excess liquid removed, and the sections mounted under a coverslip using Hydromount (National Diagnostics).

Immunohistochemistry

A rat monoclonal IgG against GATA-1 (catalog no. sc-265; Santa Cruz Biotechnology, Santa Cruz, CA) was used for immunostaining. Testes were fixed and sectioned as for in situ hybridization. Consecutive testicular sections (6 μm) were used for in situ hybridization and anti-GATA-1 staining. The sections were cleared, rehydrated through a graded alcohol series, and rinsed for 5 min in tap water. Sections were blocked in 1.5% rabbit serum in PBS for 20 min at room temperature. After blocking, sections were incubated with primary antibody diluted 1:50 in PBS overnight at 4°C and washed three times in PBS. Incubation with secondary antibody and all subsequent steps were performed using the Vectastain Elite ABC kit (catalog no. PK-6104; Vector Labs, Burlingame, CA) according to the manufacturer's instructions. Following final washes in PBS, testicular sections were incubated in DAB (catalog no. SK-4100; Vector Labs) for 5–8 min until color developed and then counterstained with hematoxylin, cleared, and mounted.

Testis and Seminal Vesicle Weights

The testes were weighed individually. Paired seminal vesicles of animals other than those used for the structural study were dissected with the coagulation gland attached. The seminal vesicle weight data provided here are from cohorts of males that are age-matched littermates. Each bar in the figure represents a single data point.

Preparation of Tissue for Microscopy

Animals at or beyond 15 days of age were killed by administration of pentobarbital and, during the perfusion procedure, used for fixation of the testis. Animals were perfused-fixed by whole-body perfusion [17]. Briefly, after i.p. administration of heparin, mice were anesthetized and the abdomen and thoracic cavity opened to expose the heart. A needle was inserted into the heart and 0.9% saline used to clear blood vessels. After clearance of vessels, a two-way valve apparatus was used to introduce 5% glutaraldehyde (EM Sciences) into vessels without removal of the needle. Animals were perfused for 25–30 min, whereupon the testes were removed, weighed, and prepared for embedding in epoxy using standard techniques [18]. Tissues were examined by both light and electron microscopy. Animals younger than 15 days of age were killed with pentobarbital and their testes excised, bisected, and immersed-fixed in 5% gluteraldehyde for 4 h. The tissue preparation for microscopy was as described above for perfused tissues.

Morphometry

The volume densities of various tissue components were determined by light microscopy of 0.92-μm thick sections using a 441-intersection grid in the ocular of the light microscope. Three fields (1332 points) were scored for each animal at 200× magnification. Points were classified as one of the following: intertubular space, Leydig cells, blood vessels, combined interstitial and tubular macrophages, unidentified interstitial components or "other," peritubular tissue, Sertoli cells, germinal elements, or tubular lumen. The intertubular space in some animals was exaggerated where swelling of this area had occurred during tissue processing. Consequently, calculations from the determinations of volume densities for

various components were undertaken in all cases without the inclusion of the intertubular region where tissue components were absent. The volume density for a particular compartment was determined by dividing the points over a desired object by the total points from the field in which the object was present. The total area occupied by an object was the product of the volume density and the testicular weight. Because the specific gravity of the testis is nearly unity, we equated the testicular weight to an equivalent volume measurement.

Cell number was determined for both Sertoli and Leydig cells for animals of 90 days of age (two wild-type and three homozygous mutant *Bclw*). Twenty serial sections (0.92 μm each) of testis were prepared from each animal. Tracings were made of five randomly selected Sertoli cells, and the combined volumes of all traced sections were calculated to yield a nuclear volume (V_n). For Leydig cells, a 441-point grid was placed over 50 randomly selected Leydig cells. The points over the nucleus (N_p) and over the cytoplasm (P_c) were then obtained, as were the total points (P_T) over both the nucleus and cytoplasm. The cell volume (V_c) was obtained for Leydig cells using the following formula:

$$V_c = N_p / V_n \times P_T$$

The mean number of Leydig cells in each group was determined by dividing the total volume of the Leydig cells by the mean volume of an individual Leydig cell.

The criteria used to stage mouse spermatogenesis were those outlined by Oakberg [19], as modified by Russell et al. [20].

Statistics

Statistics were performed with the SAS software package (SAS Institute, Inc, Clara, CA) using the General Linear Models procedure. A threshold of $P < 0.05$ was used for significance.

RESULTS

Analysis of *Bclw* Expression in Male Germ Cells and Adult Mouse Testis

We analyzed the pattern of expression of *Bclw* in germ cells during mouse spermatogenesis using Northern blot analysis of total RNA isolated from testes of mice at specific stages during prepubertal development as well as from enriched populations of haploid male germ cells. The temporal development of spermatogenesis in prepubertal mice is well established [21]. Thus, the former samples provide a reliable method of correlating cellular patterns of gene expression with the development of specific stages of male germ cells.

The RNA isolated from testes that lacked germ cells (i.e., *at/at* and *XX Sxr* mice) had the highest steady-state level of *Bclw* mRNA (Fig. 1A). This is consistent with previous reports that Bclw is expressed in postmitotic mouse Sertoli cells [5,22]. The overall steady-state level of *Bclw* mRNA is similar in testes from p7, p12, and p17 mice but is reduced in p22, even lower in p27, and lowest in adult mice (Fig. 1A). This reduction most likely reflects the decrease in the overall number of cells expressing Bclw during prepubertal development rather than a reduction in expression of *Bclw* within Sertoli cells. Because the overall signal is reduced with the onset of haploid germ cell proliferation, this suggests that *Bclw* is not expressed in haploid male germ cells. To verify this result, we performed Northern blot analysis using total RNA isolated from enriched populations of round spermatids and residual bodies (Fig. 1A). The results confirm that little, if any, *Bclw* mRNA is found in haploid round spermatid or residual bodies.

Several genes that are transcribed during the haploid stages of mouse spermatogenesis undergo a temporal delay in translation [23,24]. To exclude the possibility that any *Bclw* mRNA transcribed in diploid male germ cells was being translated in haploid germ cells, extracts of purified diploid and haploid germ cells were subjected to Western blot analysis for Bclw expression. Results (Fig. 1B) suggest that no Bclw can be detected in either round spermatids or residual bodies, the latter of which contain protein from elongating germ cells.

Sertoli cells are known to express Bclw [5,22], and Sertoli cells were the major contaminant of cell-separation preparations enriched for spermatogonia and spermatocytes. Consequently, we were unable to assess the status of expression of *Bclw* RNA in these germ cell types by this method. For this reason, we used RNA in situ hybridization as an independent method to analyze expression of *Bclw* in the testis of adult mice. We used DIG-labeled riboprobes to identify *Bclw* mRNA, because this methodology permits resolution at the single-cell level [16]. Hybridization of an antisense riboprobe derived from the 3′-UTR of a mouse *Bclw* cDNA to sections of adult wild-type mouse testis detected *Bclw* mRNA only within the basal compartment of the testis (Fig. 2A). No signal over background was detected in sections from an age-matched *Bclw* homozygous mutant animal (Fig. 2B). Interestingly, not all tubules in wild-type mice appeared to express *Bclw*, with little or no signal being observed between stages VII and VIII of the cycle (Fig. 2A). We have previously reported expression of *Bclw* in Sertoli cells purified from p18 mice [5]. To determine if *Bclw* was expressed in adult Sertoli cells, we analyzed serial sections of adult mouse testis, with either RNA in situ hybridization using the same *Bclw* antisense riboprobe or immunohistochemistry using antibodies against GATA-1, a known marker of Sertoli cells nuclei [25]. The results indicate that *Bclw* is expressed at highest steady-state levels in Sertoli cells (Fig. 2, C and D). We were unable to detect *Bclw* mRNA in spermatogonia or spermatocytes (Fig. 2C).

In summary, our results indicate that *Bclw* is expressed in postnatal Sertoli cells. If *Bclw* is expressed in adult mouse germ cells, its expression is at levels below the limit of resolution for the methods and reagents we used.

Testis and Seminal Vesicle Weights in Homozygous Mutant *Bclw* and Control Mice

No significant difference was observed in paired-testes weights between wild-type and heterozygous mutant *Bclw* littermates at all ages examined. Similarly, no significant difference was observed in the weights of paired testes from homozygous mutant *Bclw* animals compared to control (wild-type or heterozygous mutant) animals between p9 and p23 (Fig. 3A). However, beginning at p34, weights of paired testes from homozygous mutant *Bclw* animals were always significantly less than those from control littermates. By 9 mo of age, paired-testes weights from homozygous mutant *Bclw* animals were dramatically reduced, being only 12%–20% of those from control animals (Fig. 3A).

Seminal vesicle weights were measured in adult animals from 3 to 15 mo of age (Fig. 3B). A trend toward decreasing seminal vesicle weights was first noticed between 7 and 7.5 mo. From 7.5 mo onward, seminal vesicle weights declined progressively to approximately 10% of their normal weight at 12 mo of age.

Comparative Histopathology of Homozygous Mutant *Bclw* and Control Littermates: The Interstitial Compartment

Leydig cells—No significant difference was observed in the distribution and appearance of fetal Leydig cells in homozygous mutant *Bclw* and control animals studied at p9, p17, and p20 (Fig. 4, A and B). Similarly, both the Leydig cells that arose during pubertal development and the adult generation of Leydig cells also appeared normal by light

microscopy in young animals. The volume of the Leydig cell compartment did not appear to differ between Bclw-deficient animals and their age-matched controls during prepubertal development (Fig. 3C). In contrast, by 3 mo of age, a subjective analysis by light microscopy (Fig. 4, C and D) suggested an increase in the Leydig cell compartment in homozygous mutant *Bclw* animals that was confirmed by morphometry (Fig. 3C). In animals between 3 and 8 mo of age, the total volume of the Leydig cell compartment in homozygous mutants was almost twice as large as that in control, age-matched littermates (Fig. 3C). However, measurement of Leydig cell size in 3-mo-old mutant (mean value of 1786.6 ± 164.3) and control animals (mean value of 1826.8 ± 196.7) suggested no difference in the size of individual Leydig cells. The number of Leydig cells in wild-type animals was 13.346 ± 0.725 million, and the number in *Bclw* mutants was 21.582 ± 0.883 million. Thus, hyperplasia, and not hypertrophy, appears to be the mechanism underlying the increase in volume of the Leydig cell compartment. Histological examination (Fig. 4F) and morphometric analysis of testes from Bclw-deficient mice older than 8 mo provided visual and semiquantitative, but obvious, evidence for a gradual loss in Leydig cells until 12 mo of age, by which time very few or no Leydig cells could be found (Fig. 4G). In contrast, the Leydig cell population in control animals remained relatively stable at all ages (Fig. 3C).

Ultrastructural examination of Leydig cells in homozygous mutant *Bclw* animals revealed a normal appearance during prepubertal development and up to approximately 7 mo of age (Fig. 5A). However, in mutants 8 mo and older, Leydig cells were occasionally found undergoing apoptosis (Fig. 5B). The apoptotic cells were identified as Leydig cells based on the distinctive morphology of the mitochondria and the abundant, smooth endoplasmic reticulum [26]. Leydig cells undergoing apoptosis were occasionally observed in the process of being surrounded or phagocytosed by interstitial macrophages (Fig. 5C).

Blood vessels—No consistent difference was observed in the volume of the vascular compartment in developing and adult mutant and control animals as a function of age (Fig. 3D). However, the volume of the vascular system appeared to differ (i.e., to be larger) when compared with *Bclw* mutants at some ages.

Other interstitial cells—In homozygous mutants 1 mo of age and older, the interstitial compartment contained a variety of cells not commonly seen in controls, some of which could not be identified by light microscopy. However, by electron microscopy, these cells often proved to be monocytic in appearance and were not observed in the age-matched, control littermates (Fig. 5A). Ultrastructural analysis suggested that the majority of these cells fell into three categories: 1) macrophages, both activated and inactivated forms, with the activated forms containing abundant phagocytosed material; 2) mast cells (rare); and 3) mesenchymal-appearing cells. For quantitative purposes, except for the macrophages, the aforementioned cells were considered as “interstitial other.” There was no consistent difference in the volume of the compartment of unidentified cells termed “interstitial other” in homozygous mutant *Bclw* and control, age-matched animals of up to 8 mo of age (Fig. 3E). An apparent increase in the relative volume of these cell types was observed in homozygous mutant mice between 9 and 12 mo of age. Macrophages appeared to increase their relative volume on a consistent basis from 1 mo onward, although macrophage relative volumes were not recorded specifically for the interstitial compartment.

Comparative Histopathology of Homozygous Mutant *Bclw* and Control Littermates: The Tubular Compartment

Germ cells—Evidence of abnormal germ cell degeneration in homozygous mutant males was first observed at p20 (Fig. 4, A and B). Cell degeneration appeared to affect all types of germ cells; however, massive degeneration of elongated spermatids arrested at step 13 of

development was noted at p34 (Fig. 6). The overall effect of this pattern of cell degeneration led to a reduction in the number of spermatogonia, spermatocytes, and round spermatids and a near or complete absence of germ cells past step 13 of spermiogenesis. Degenerating germ cells in homozygous mutants were phagocytosed by Sertoli cells. At p34, symplasts of round spermatids were also observed (Fig. 6A). Germ cell degeneration continued to deplete the epithelium during late prepubertal development and in adult animals. In mutants older than 7 mo, only a few spermatogonia were found among the sparse population of remaining Sertoli cells (Fig. 4, F and G; see next section).

Sertoli cells—In wild-type and heterozygous mutant *Bclw* animals, the relative volume of the Sertoli cell nuclear compartment increased during development (i.e., until p43–90) and, thereafter, appeared to be relatively stable throughout the period studied (Fig. 3F). There appeared to be no difference in the relative volume of the Sertoli cell nuclear compartment in mutants and control animals between p9 and p20. However, beginning at p23, the volume of this compartment was significantly less in homozygous mutants compared to controls. By p90, a greater than 60% relative reduction was observed in the total volume of the Sertoli cell nuclear compartment in homozygous mutants compared to controls. This reduction increased with time until the Sertoli relative nuclear volume approached or, in some cases, reached zero at 12 mo of age (Fig. 3F). Morphometric data obtained for animals 90 days of age revealed no difference in the size of Sertoli cell nuclei throughout this period (data not shown), indicating that the decrease resulted from reduced numbers of Sertoli cells.

From a qualitative standpoint, most Sertoli cells in homozygous mutants showed normal ultrastructural features, although some showed nuclear vacuolation (Fig. 7A) and mitochondrial swelling (Fig. 7, A and C). Interestingly, regardless of age, Sertoli cells in Bclw-deficient animals never displayed chromatin condensation on the circumference of the nucleus, nor did they show nuclear condensation and fragmentation. The ultrastructure of Sertoli cells in p90 Bclw-deficient mice suggested that they had maintained an intact Sertoli cell barrier. Evidence to support this conclusion includes linear electron opacities in the Sertoli-Sertoli junctional regions that are characteristic of membrane fusion in these animals (Fig. 7B). Although only a small fraction of Sertoli-Sertoli junctions could be examined using this technique, the results were consistent. In contrast, in animals 5.5 mo and older, Sertoli cell detachment from the basal lamina was noted (Fig. 7, C and D), making the loss of the functional integrity of the barrier obvious. In many cases, contact by adjacent Sertoli cells via their lateral surfaces was lost, representing clear evidence for the disruption of the Sertoli cell barrier (Fig. 7C).

In adult homozygous mutants of all ages, a small number of Sertoli cells detached from the basal lamina and formed “balls,” as previously described in c-*kit* mutant mice both before and following transplantation of germ cells [27]. Such balls of Sertoli cells were never observed in testes from wild-type or heterozygous mutants. Occasional Sertoli cells displayed degenerative features in *Bclw* mutant mice between 3 and 7 mo of age, but such features were evident in all such animals older than 7 mo. Sertoli cells were observed that had detached from the basal lamina (Fig. 8A), that had increased in cytoplasmic density, and that were located in the center of the tubule. Such “densified” cells were identified as Sertoli cells based on their mitochondria [28].

In animals 5.5 mo and older, dying or dead Sertoli cell masses occupied a large space in the center of the tubule (Figs. 4E and 8A). Macrophages entered the tubule (Fig. 8C) to form the foreign-body giant cells (Fig. 9, A and B) that actively phagocytosed the centrally located, densified Sertoli cells. As Sertoli cell loss progressed, the tunica propria with the innermost basal lamina became either partially free (Figs. 7, C and D; 8, A and B; and 9C) or completely free of cellular contact. Although considerable animal-to-animal variability was

observed, peritubular cell ghosts were the most commonly encountered seminiferous tubular profile (Figs. 4G and 9D).

It was difficult to resolve germ from Sertoli cells in our morphometric determinations. Consequently, the relative volumes of these two cell types (i.e., Sertoli cell cytoplasm and germ cells) were combined and termed “remainder” to distinguish them from those determinations made for Sertoli cell nuclei. Similar to the timing of the onset of germ cell degeneration and reduction in the volume of the Sertoli nuclear compartment, the “remainder” relative volume in homozygous mutants first began to differ from that in control animals between p20 and p23 (Fig. 3G). After p23, the relative volume of this compartment declined progressively until 12 mo of age, when it was approximately 1% of normal. In contrast, in control animals, the combined volumes of Sertoli cell cytoplasm and germ cells increased steadily during pubertal development and remained stabilized at 1 yr of age (Fig. 3G).

Tubular lumen—The volume of the tubular lumen compartment increased sharply in p34 control animals and remained relatively stable in adult animals. In contrast, a dramatically smaller tubular lumen volume was observed in the testes of both developing and adult homozygous mutant *Bclw* males compared to control littermates (Fig. 3H). The data shown in Figure 3H appear to suggest that the volume of the lumen compartment in homozygous mutants 7 mo and older is larger than that in p43–180 animals. However, *lumen* was defined as being anything internal to the peri-tubular cell ghosts. Thus, this larger lumen in the older homozygous mutants is an artifact that results from the absence of Sertoli cells.

Intertubular macrophages—Interstitial macrophages were abundant in the testes of adult *Bclw* mutants, and from the extent of engulfed material, they appeared to phagocytose extratubular material. Macrophages were observed within the lumen of seminiferous tubule in mutants as young as 5.5 mo of age, although they were never found in control animals. In animals 5.5 mo of age, intertubular macrophages apparently fused to form foreign-body giant cells (Fig. 9, A and B), which appeared to engulf and phagocytose the dying/dead intratubular Sertoli cells. In some tubules, foreign-body giant cells were the only cell type remaining within the tubular lumen following the loss of germ cells and Sertoli cells (Figs. 4, F and G, and 9A).

The relative volume of the macrophage compartment (i.e., macrophages both within and outside of the seminiferous tubules of normal animals) was routinely increased in homozygous mutant animals (Fig. 3I). In 8- to 12-mo-old animals, total (i.e., intra- and extratubular) macrophage relative volume was approximately eightfold increased in homozygous mutants compared with control, age-matched littermates (Fig. 3I).

Peritubular tissue—No significant difference was observed in the relative volume of the peritubular tissue compartment in homozygous mutant and control animals as a function of age (Fig. 3J). Electron microscopy revealed that the peritubular tissue in homozygous mutants appeared to be infolded and thickened, as is commonly seen in animals whose tubules are small because of the depletion of germ cells (Fig. 9D). The innermost basal lamina was duplicated. After depletion of Sertoli and germ cells, the peritubular cells were the only remnants of the seminiferous tubules (Figs. 4G and 9D).

DISCUSSION

We have performed detailed histologic, cytologic, and morphometric analyses of the onset, progression, and presumed end point of testicular degeneration in Bclw-deficient mice. This study extends previous findings regarding testicular degeneration in these animals [5,22].

Specifically, we have quantified the successive changes in populations of testicular cells in *Bclw*-mutant and control animals from shortly after birth to more than 1 yr of age. In addition, we have used Northern and Western blot analyses and in situ hybridization to correct and refine our knowledge regarding the pattern of Bclw expression in adult mouse testis. Together, these data enable us to develop models for the function of Bclw during male germ cell development and provide novel insight regarding the role of the Sertoli cell in regulating adult testicular homeostasis.

Pattern of Expression of Bclw in Adult Mouse Testis

The null mutant allele of *Bclw* in the ROSA41 strain of mice was generated using a retroviral gene trap system [5,10]. With this particular system, transcriptional activity of the mutated gene in different cells of mice can be detected using the RNA splice acceptor-bacterial β-galactosidase (*lacZ*) function of the gene trap vector in conjunction with X-gal staining. Using this criterion, one of our group (G.R.M.) previously reported expression of *Bclw* in Sertoli cells and elongate germ cells in adult mice [5]. Two additional methods were used to determine whether the β-gal activity reflected the pattern of *Bclw* gene expression in testis. First, Western blot analysis was performed on purified mouse Sertoli cells using two independent, affinity-purified antisera that had been generated against synthetic peptides from the NH_2 and COOH termini of mouse Bclw. Second, immunohistochemistry was performed using testicular histopathology from wild-type and homozygous mutant ROSA41 animals using the same antipeptide antisera. The results supported the data generated by X-gal staining: that *Bclw* was expressed in both Sertoli cells and elongate germ cells [5].

In contrast to these findings, another study used RNA in situ hybridization to demonstrate that *Bclw* transcripts were not found at significant levels in elongate spermatids or mature sperm but were, instead, found at highest levels in spermatogonia, with lower levels in Sertoli cells [22]. Significantly, no evidence was found for expression of Bclw in Leydig cells based on in situ hybridization and Western blot analysis of protein from an established Leydig cell line.

To understand the mechanism for development of a mutant phenotype in an organ requires knowledge regarding the cellular pattern of expression of the gene product in question. Such information is particularly important when the gene is expressed in both the germ cell and the supporting somatic cells in a gonad, which is the case with testicular expression of *Bclw*. The present study suggests that *Bclw* is not transcribed, and that Bclw protein is not found in haploid germ cells. This indicates that the expression of β-gal in elongate germ cells in ROSA41 mice does not reflect expression of the mutated *Bclw* gene within this specific cell type [5].

The ROSAβ-gal provirus used to generate this mutant allele of Bclw contains a phosphoglycerate kinase gene promoter-neomycin phosphotransferase gene (PGK-neo) cassette, which serves as a selectable marker following infection of embryonic stem cells [10]. Two recent reports have demonstrated convincingly that integration of this minigene within a transcription unit can influence expression of the transcription unit itself [29,30]. Thus, the erroneous expression of *lacZ* observed in elongate germ cells in heterozygous $Bclw^{Gtrosa41}$ may be due to the PGK-neo cassette in this mutant allele. We also conclude that the two independent, affinity-purified peptide antisera used in this previous study may have cross-reacted with a nonspecific antigen, which is found in elongate germ cells of wild-type but not homozygous mutants.

We used in situ hybridization with DIG-labeled probes to evaluate expression of *Bclw* mRNA in adult mouse testis. Our results confirmed that Sertoli cells express *Bclw*. In contrast to previous reports [22,31], we could find no evidence of *Bclw* mRNA in

spermatogonia. The level of expression of *Bclw* mRNA in diploid male germ cells may have been below the limits of sensitivity for the in situ assay we used.

In summary, the results from this and previous studies are in agreement that Bclw is expressed in Sertoli cells, but not at appreciable levels in haploid germ cells, in adult mice. Bclw has also been reported to be expressed in adult [22,31] and prepubertal [32] diploid male germ cells in rodents, although we were unable to detect this during the present study using in situ hybridization.

Interpretation of the Timing and Pattern of Germ Cell Loss in Bclw Mutants

Consideration of the expression pattern of *Bclw* in the testis, and of the timing and extent of male germ cell death during postnatal development of Bclw-deficient animals, enables the formation of models regarding the function of *Bclw* in murine spermatogenesis and the mechanism of germ cell loss in *Bclw*-deficient mice.

Germ cell loss from Bclw-deficient male mice was categorized in two discrete classes. First, death of spermatogonia, spermatocytes, and round spermatids was sporadic. That is, degenerating cells were found in tubules without regard to cycle stage, and they were found not to degenerate in clones. Assuming that *Bclw* is expressed in diploid male germ cells, the sporadic death of spermatogonia and spermatocytes may be a direct consequence of loss of Bclw function in these cells. Alternatively, loss of these cells types may result from dysfunctional Bclw-deficient Sertoli cells. However, because *Bclw* does not appear to be expressed in haploid germ cells, it is doubtful that the death of round spermatids results from loss of *Bclw* function in this cell type. Instead, it appears to be more probable that the multinucleation and death of round spermatids results from Bclw-deficient Sertoli cell dysfunction.

The second form of germ cell death was a nonsporadic arrest and stage-specific degeneration of elongating spermatids. At step 13 of spermiogenesis, virtually 100% of step 13 spermatids underwent a synchronous (i.e., clonal) process of cell death. During this process, cytoplasmic bridges were lost, and the cytoplasm of clonal cells rounded up and densified. As with round spermatids, the absence of *Bclw* expression in elongate spermatids makes it likely that loss of this cell type results from Sertoli cell dysfunction. Interestingly, mice deficient in Desert hedgehog (Dhh) or retinoid X receptor beta (RXRβ) also display defects in germ cell development during the late stages of spermio-genesis [33,34]. Germ cells in *Dhh* mutant mice arrest at step 15, whereas those in *RXRβ* mutant mice complete differentiation but fail to undergo spermiation. As with Bclw, neither Dhh or RXRβ is expressed in elongating spermatids, although both are expressed in Sertoli cells [33,34]. Thus, arrest during elongate spermatid development in these mutants presumably results from the loss of gene function in Sertoli or other somatic cells, although the mechanism responsible for such arrest is currently unclear. Experiments are underway to determine whether germ cells have an intrinsic requirement for *Bclw* during spermatogenesis by transplantation of Bclw-deficient male germ cells into a wild-type testicular environment using the spermatogonial transplantation techniques pioneered by Brinster and colleagues [35].

Loss of Sertoli Cells in Bclw-Deficient Mice

Clearly, *Bclw* is expressed in adult Sertoli cells [5,22,31,32]. Moreover, *Bclw* is also required for long-term survival of Sertoli cells in the normal adult mouse [5,22]. In the present study, an apparent increase in numbers of degenerating germ cells was first observed in the testes of homozygous mutant *Bclw* mice at p20. This is consistent with previous findings regarding timing of the onset of germ cell degeneration in Bclw-deficient animals

[5,22]. Significantly, in the present study, an effect of loss of Bclw function on the Sertoli cell population also first manifested at p20–23. We are unaware of a precedence for loss of male germ cells in mice causing extensive depletion of Sertoli cells. Indeed, loss of all germ cells leads to what is commonly called “Sertoli cell-only syndrome.” Consequently, loss of Sertoli cells at p20–23 likely is the direct result of a deficiency of Bclw within this cell type. We are currently testing this hypothesis by analysis of long-term survival of Sertoli cells in Bclw-deficient mice, which lack germ cells from birth.

During normal mouse development, Sertoli cells complete exit from mitosis by p17 [2]. It is interesting that an effect on the Sertoli cell population in Bclw-deficient mice is first noted shortly after this time. Bclw is expressed in mitotic Sertoli cells in the neonatal rodent [31]. We found no evidence for loss of Sertoli cells in Bclw-deficient mice before their exit from mitosis. Thus, it appears that the death-protecting function of Bclw is only required in post-mitotic Sertoli cells, and that other death-protecting members of the Bcl2 family or survival-signaling molecules can sustain mitotic, Bclw-deficient Sertoli cells.

Bclw-deficient mice provide a unique opportunity to observe the characteristics of cellular degeneration associated with Sertoli cells in vivo. Sertoli cells are often removed from the basal lamina during early adulthood in several mutant strains of mice, including Bax-deficient [36] (unpublished results), kit-ligand-deficient [27], and several others (unpublished results). However, despite loss of contact with the basal lamina, these balls of Sertoli cells do not appear to undergo apoptosis but, instead, remain viable yet structurally abnormal [27] (unpublished results).

Such balls of Sertoli cells were occasionally observed in Bclw-deficient animals. In addition, in other Sertoli cells that lost contact with the basal lamina, the cytoplasm appeared to be greatly densified, and the cell became positioned centrally within the seminiferous tubule. The densification observed within Bclw-deficient Sertoli cells has not been observed in Sertoli cells from Bax-deficient, kit-deficient, or several other lines of mutant mice with defective spermatogenesis (unpublished results). Sertoli cells in Bclw-deficient animals ultimately degenerated and were phagocytosed. However, while degenerating, they did not display all of the classical features normally associated with apoptosis, such as chromatin condensation on the nuclear envelope and shrinkage and fragmentation of the nucleus. Instead, the cytoplasm of Bclw-deficient Sertoli cells appeared to condense, and whereas evidence was found of mitochondrial swelling, cytoplasmic organelles remained relatively intact. In addition, the demise of Bclw-deficient Sertoli cells was not immediately accompanied by phagocytosis of the dying cells by other Sertoli cells. Instead, macrophages in the form of foreign-body giant cells invaded the seminiferous tubules to ingest the massive amount of Sertoli cell debris formed by the loss of the entire population of Sertoli cells. We are unaware of any other cases in which macrophages enter the seminiferous tubule.

A major question that arises from this study is why Bclw-deficient Sertoli cells die over such an extended period of time in vivo. Apoptosis is usually a rapid and efficient process, as is required for effective remodeling of tissues during embryogenesis or removal of potentially dangerous, precancerous cells. Indeed, mitotic Sertoli cells are competent to undergo apoptosis within a few hours either following x-irradiation in vivo [37] or after explant in vitro [38]. In contrast, postmitotic Sertoli cells are resistant to x-irradiation [39,40]. Neither wild-type or Bclw-deficient postmitotic Sertoli cells display classical features of apoptosis (i.e., margination of the chromatin against the nuclear membrane, condensation of the nucleus and cytoplasm, fragmentation of the nucleus, and formation of apoptotic bodies [41]) in vivo following release from the basement membrane. Thus, prolonged survival of such Sertoli cells in vivo may, at least in part, result from their postmitotic status. The

densification of the cytoplasm and swelling of the mitochondria observed in Bclw-deficient Sertoli cells, but not in wild-type Sertoli cells, is likely a direct consequence of the loss of function of Bclw in this cell type, which could produce an imbalance in death-protecting Bcl2 family members, such as Bax. An imbalance in levels of Bax activity in mammalian cells often leads to apoptosis. Interestingly, the ability of Bax to mediate classical apoptosis in mammalian cells in vitro can be blocked by inclusion of caspase inhibitors [42]. In such cases, chromatin condensation and nuclear fragmentation is inhibited, although caspase-independent activities of Bax, including a fall in the mitochondrial membrane potential and mitochondrial swelling, still occur, which ultimately leads to cell death [42]. Thus, one possibility is that Bclw-deficient post-mitotic Sertoli cells might also fail to undergo classical apoptosis due to a failure to produce or activate caspases. Additional possibilities for the protracted loss of Bclw-deficient postmitotic Sertoli cells include a gradual, age-related decline in expression of other death-protecting molecules.

Changes in the Leydig Cell Compartment of Bclw-Deficient Mice

Leydig cells initially become hyperplastic after changes have occurred in the compartment volumes of the germ and Sertoli cells [5]. This is a normal response to elevated levels of gonadotropins, which are expected to rise due to a deficiency in spermatogenesis. However, by approximately 7 mo of age, fewer Leydig cells are present in homozygous mutant animals than in controls. This trend continues until 11 mo of age, at which time Leydig cells are essentially absent from homozygous mutant animals. Interestingly, the decrease in the Leydig cell compartment is observed when few, if any, Sertoli cells remain in the seminiferous tubules. Literature is accumulating that suggests the size of the Leydig cell population is influenced by the size of the Sertoli cell population [43–46]. Loss of Leydig cells in aged, Bclw-deficient males appears to be an apoptotic event, because several classic morphological features of apoptosis are observed: condensation of chromatin on the nuclear envelope, fragmentation of the nucleus, shrinkage of the cell, and phagocytosis by adjacent macrophages. Rarely has apoptosis been noted in Leydig cells, because this population is usually relatively stable in wild-type animals. Perhaps the most notable example is following administration of rats with ethane dimethane sulfonate (EDS), which results in loss of the adult Leydig cell population via apoptosis [47]. However, unlike the situation using EDS, Leydig cells in Bclw-deficient animals do not regenerate.

These findings support a role for Sertoli cells in regulation of adult testicular homeostasis. Specifically, Sertoli cells may provide signals that regulate proliferation and survival of Leydig cells in adult mice. Two attractive candidates for such signaling mechanisms are the kit-ligand/kit-receptor and Hedgehog/Patched ligand-receptor pathways. Kit ligand is produced by Sertoli cells; kit receptor is expressed by both germ and Leydig cells [48]. Kit ligand may be a survival factor for both adult and immature Ley-dig cells [49]. *Desert hedgehog* is expressed only by Sertoli cells in the testis, whereas the *Patched-1* receptor is likely expressed in Leydig cells [33,50]. On a mixed genetic background, *Dhh*-mutant mice lack adult Leydig cells [50]. It will be of interest to determine whether introduction of exogenous Desert hedgehog or kit ligand in Sertoli cell-depleted testes of aged, Bclw-deficient mice is sufficient to mediate repopulation of Leydig cells from the lymphatic endothelium.

Bclw-deficient mice provide a unique opportunity to analyze the consequence of loss of Sertoli cells on adult testicular homeostasis. Future experiments should provide novel insight regarding the molecular and cellular mechanisms involved in regulating adult Leydig cell homeostasis.

Acknowledgments

We thank Bruce L. Tetzlaff for help with the statistical analysis, Ying Li and Angie Raymer for technical assistance, Neville Whitehead for animal husbandry, and Mary Ann Handel for comments on the manuscript as well as support and advice on cell-separation techniques.

References

1. Capel B. The battle of the sexes. Mech Dev 2000;92:89–103. [PubMed: 10704890]
2. Vergouwen RPFA, Jacobs SGPM, Huiskamp R, Davids JAG, de Rooij DG. Proliferative activity of gonocytes, Sertoli cells and interstitial cells during testicular development in mice. J Reprod Fertil 1991;93:233–243. [PubMed: 1920294]
3. Steinberger A, Steinberger E. Replication pattern of Sertoli cells in maturing rat testis in vivo and in organ culture. Biol Reprod 1971;4:84–87. [PubMed: 5110903]
4. Russell LD, Bartke A, Goh JC. Postnatal development of the Sertoli cell barrier, tubular lumen, and cytoskeleton of Sertoli and myoid cells in the rat, and their relationship to tubular fluid secretion and flow. Am J Anat 1989;184:179–189. [PubMed: 2750675]
5. Ross A, Waymire KG, Moss JE, Parlow AF, Skinner MK, Russell LD, MacGregor GR. Testicular degeneration in Bclw-deficient mice. Nat Genet 1998;18:251–255. [PubMed: 9500547]
6. Minn AJ, Swain RE, Ma A, Thompson CB. Recent progress on the regulation of apoptosis by Bcl-2 family members. Adv Immunol 1998;70:245–279. [PubMed: 9755339]
7. Chao DT, Korsmeyer SJ. Bcl2 family: regulators of cell death. Annu Rev Immunol 1998;16:395–419. [PubMed: 9597135]
8. Antonsson B, Martinou JC. The Bcl2 protein family. Exp Cell Res 2000;256:50–57. [PubMed: 10739651]
9. Tsujimoto Y, Shimizu S. Bcl2 family: life-or-death switch. FEBS Lett 2000;466:6–10. [PubMed: 10648802]
10. Friedrich G, Soriano P. Promoter traps in embryonic stem cells: a genetic screen to identify and mutate developmental genes in mice. Genes Dev 1991;5:1513–1523. [PubMed: 1653172]
11. Bellvé AR, Millette CF, Bhatnagar YM, O'Brien DA. Dissociation of the mouse testis and characterization of isolated spermatogenic cells. J Histochem Cytochem 1977;25:480–494. [PubMed: 893996]
12. Bellvé AR. Purification, culture, and fractionation of spermatogenic cells. Methods Enzymol 1993;225:84–113. [PubMed: 8231890]
13. Chomczynski P, Saachi N. Single-step method of RNA isolation by acid guanidinium thiocyanate-phenol-chloroform extraction. Anal Biochem 1987;162:156–159. [PubMed: 2440339]
14. Ausubel, FM.; Brent, R.; Kingston, RE.; Moore, DD.; Seidman, JG.; Smith, JA.; Struhl, K. Current Protocols in Molecular Biology. New York: Wiley Interscience; 1994.
15. Cobb J, Cargile B, Handel MA. Acquisition of competence to condense metaphase I chromosomes during spermatogenesis. Dev Biol 1999;205:49–64. [PubMed: 9882497]
16. Wilkinson, DG.; Nieto, MA. Detection of mRNA by in situ hybridization to tissue sections and whole mounts. In: Wassarman, PM.; De-Pamphilis, ML., editors. Methods in Enzymology, vol 225: Guide to Techniques in Mouse Development. San Diego: Academic Press; 1993. p. 361-373.
17. Sprando, RL. Perfusion of the rat testis through the heart using heparin. In: Russell, LD.; Ettlin, RA.; Sinha Hikim, AP.; Clegg, ED., editors. Histological and Histopathological Evaluation of the Testis. Vienna, IL: Cache River Press; 1990. p. 277-280.
18. Russell LD, Burguet S. Ultrastructure of Leydig cells as revealed by secondary tissue treatment with a ferrocyanide-osmium mixture. Tissue Cell 1977;9:751–766. [PubMed: 205012]
19. Oakberg EF. A description of spermiogenesis in the mouse and its use in analysis of the cycle of the seminiferous epithelium and germ cell renewal. Am J Anat 1956;99:391–414. [PubMed: 13402725]
20. Russell, LD.; Ettlin, RA.; Sinha Hikim, AP.; Clegg, ED. Histological and Histopathological Evaluation of the Testis. Vienna, IL: Cache River Press; 1990.

21. Nebel BR, Mamarose AP, Hackett EM. Calendar of gametic development in the prepuberal male mouse. Science 1961;134:832–833. [PubMed: 13728067]
22. Print CG, Loveland KL, Gibson L, Meehan T, Stylianou A, Wreford N, de Kretser D, Metcalf D, Kontgen F, Adams JM, Cory S. Apoptosis regulator Bclw is essential for spermatogenesis but appears otherwise redundant. Proc Natl Acad Sci U S A 1998;95:12424–12431. [PubMed: 9770502]
23. Braun RE, Peschon JJ, Behringer RR, Brinster RL, Palmiter RD. Protamine 3′-untranslated sequences regulate temporal translational control and subcellular localization of growth hormatids of transgenic mice. Genes Dev 1989;3:793–802. [PubMed: 2744463]
24. Hecht NB. Regulation of ‘haploid expressed genes’ in male germ cells. J Reprod Fertil 1990;88:679–693. [PubMed: 2182846]
25. Yomogida K, Ohtani H, Harigae H, Ito E, Nishimune Y, Engel JD, Yamamoto M. Developmental stage- and spermatogenic cycle-specific expression of transcription factor GATA-1 in mouse Sertoli cells. Development 1994;120:1759–1766. [PubMed: 7924983]
26. Russell, LD. Leydig cell structure. In: Payne, AH.; Hardy, MP.; Russell, LD., editors. The Leydig Cell. Vienna, IL: Cache River Press; 1995. p. 43-96.
27. Parreira GG, Ogawa T, Avarbock MR, Franca LR, Brinster RL, Russell LD. Development of germ cell transplants in mice. Biol Reprod 1998;59:1360–1370. [PubMed: 9828179]
28. Russell LD, Brinster RL. Transplants of rat spermatogonia into mice seminiferous tubules: preliminary ultrastructural observations 17. J Androl 1996;17:615–627. [PubMed: 9016391]
29. Gerard M, Hernandez L, Wevrick R, Stewart CL. Disruption of the mouse necdin gene results in early post-natal lethality. Nat Genet 1999;23:199–202. [PubMed: 10508517]
30. Kissel H, Timokhina I, Hardy MP, Rothschild G, Tajima Y, Soares V, Angeles M, Whitlow SR, Manova K, Besmer P. Point mutation in kit receptor tyrosine kinase reveals essential roles for kit signaling in spermatogenesis and oogenesis without affecting other kit responses. EMBO J 2000;19:1312–1326. [PubMed: 10716931]
31. Yan W, Samson M, Jegou B, Toppari J. Bclw forms complexes with Bax and Bak, and elevated ratios of Bax/Bcl-w and Bak/Bcl-w correspond to spermatogonial and spermatocyte apoptosis in the testis. Mol Endocrinol 2000;14:682–699. [PubMed: 10809232]
32. Yan W, Suominen J, Samson M, Jégou B, Toppari J. Involvement of Bcl2 family proteins in germ cell apoptosis during testicular development in the rat and pro-survival effect of stem cell factor on germ cells in vitro. Mol Cell Endocrinol 2000;165:115–129. [PubMed: 10940490]
33. Bitgood MJ, Shen L, McMahon AP. Sertoli cell signaling by Desert hedgehog regulates the male germline. Curr Biol 1996;6:298–304. [PubMed: 8805249]
34. Katner P, Mark M, Leid M, Gansmuller A, Chin W, Grondona JM, Décimo D, Krezel W, Dierich A, Chambon P. Abnormal spermatogenesis in RXRβ mutant mice. Genes Dev 1996;10:80–92. [PubMed: 8557197]
35. Brinster RL, Zimmerman JW. Spermatogenesis following male germ-cell transplantation. Proc Natl Acad Sci U S A 1994;91:11298–11302. [PubMed: 7972053]
36. Knudson CM, Tung KS, Tourtellotte WG, Brown GA, Korsmeyer SJ. Bax-deficient mice with lymphoid hyperplasia and male germ cell death. Science 1995;270:96–99. [PubMed: 7569956]
37. Allan DJ, Gobé GC, Harmon BV. Sertoli cell death by apoptosis in the immature rat testis following x-irradiation. Scanning Microsc 1988;2:503–512. [PubMed: 3368774]
38. Dirami G, Ravindranath N, Kleinman HK, Dym M. Evidence that basement membrane prevents apoptosis of Sertoli cells in vitro in the absence of known regulators of Sertoli cell function. Endocrinology 1995;136:4439–4447. [PubMed: 7664664]
39. Harding LK. The survival of germ cells after irradiation of the neonatal male rat. Int J Radiat Biol 1961;3:539–551. [PubMed: 13711488]
40. Erickson BH, Blend MJ. Response of the Sertoli cell and stem germ cell to ^{60}Co γ irradiation (dose and dose rate) in the testis of immature rats. Biol Reprod 1976;14:641–650. [PubMed: 1276328]
41. Wylie AH, Kerr JFR, Currie AR. Cell death: the significance of apoptosis. Int Rev Cytol 1980;68:251–306. [PubMed: 7014501]

42. Xiang J, Chao DT, Korsmeyer SJ. BAX-induced cell death may not require interleukin 1β-converting enzyme-like proteases. Proc Natl Acad Sci U S A 1996;93:14559–14563. [PubMed: 8962091]
43. Kerr JB, Sharpe RM. Stimulatory effect of follicle-stimulating hormone on rat Leydig cells. A morphometric and ultrastructural study. Cell Tissue Res 1985;239:405–415. [PubMed: 3919952]
44. Van Haaster LH, de Jong FH, Docter R, de Rooij D. The effect of hypothyroidism on Sertoli cell proliferation and differentiation and hormone levels during testicular development in the rat. Endocrinology 1992;131:1574–1576. [PubMed: 1505485]
45. França LR, Silva VA Jr, Chiarini-Garcia H, Garcia SK, Russell LD. L. D. Cell proliferation and hormonal changes during post-natal development of the testis in the pig. Biol Reprod 63:1629–1636. [PubMed: 11090429]
46. França LR, Hess R, Cook P, Russell LD. Neonatal hypothyroidism causes delayed Sertoli cell maturation in rats treated with propylthio-uracil: evidence that the Sertoli cell dictates testis growth. Anat Rec 1995;242:57–69. [PubMed: 7604982]
47. Kerr JB, Bartlett JM, Donachie K. Acute response of testicular interstitial tissue in rats to the cytotoxic drug ethane dimethanesulphonate. An ultrastructural and hormonal assay study. Cell Tissue Res 1986;243:405–414. [PubMed: 3004734]
48. Loveland KL, Schlatt S. Stem cell factor and c-kit in the mammalian testis: lessons originating from Mother Nature's gene knockouts. J Endocrinol 1997;153:337–344. [PubMed: 9203987]
49. Yan W, Kero J, Huhtaniemi I, Toppari J. Stem cell factor functions as a survival factor for mature Leydig cells and a growth factor for precursor Leydig cells: implication of a role of the stem cell factor/c-Kit system in Leydig cell development. Dev Biol 2000;227:169–182. [PubMed: 11076685]
50. Clark AM, Garland KK, Russell LD. Desert hedgehog (*Dhh*) gene is required in the mouse testis for formation of adult-type Leydig cells and normal development of peritubular cells and seminiferous tubules. Biol Reprod 2000;63:1825–1838. [PubMed: 11090455]

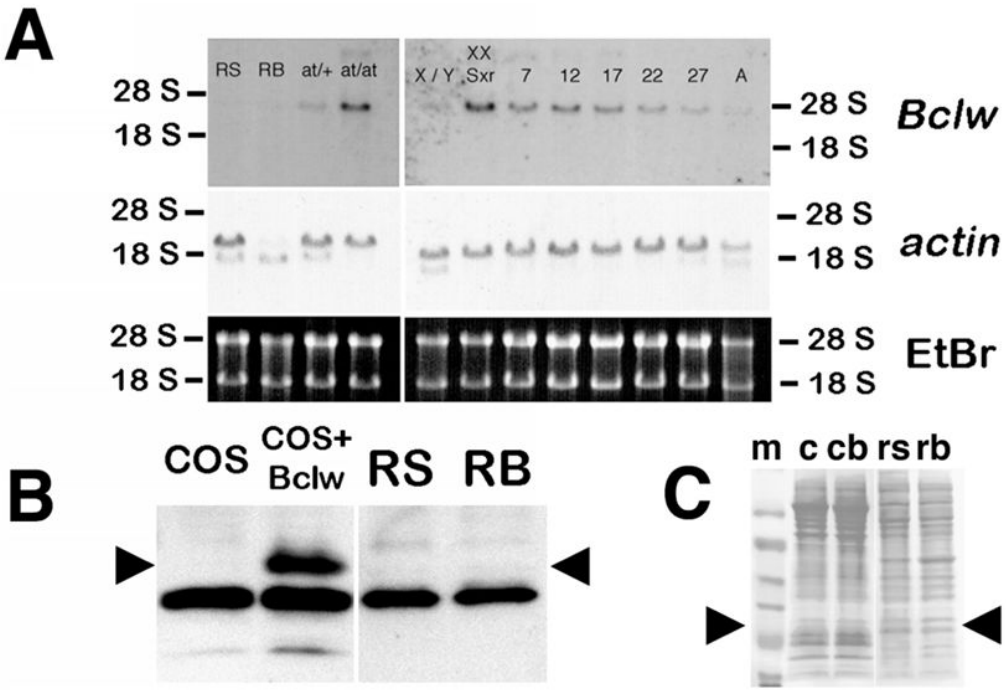

FIG. 1.

Expression of *Bclw* mRNA and protein in male mouse germ cells. **A**) RNA was extracted from preparations of enriched germ cells, from testes of heterozygous or homozygous mutant *atrichosis* (*at*) mice, from testes of normal (X/Y) or sex-reversed mice (*XX Sxr*), or from testes of mice at Postnatal Day 7, 12, 17, 22, and 27 during prepubertal development and from adults. The percentage of contaminants in the enriched germ cell preparations is as described in *Materials and Methods.* Testes from *at/at* and *XX Sxr* animals contain extremely few or no germ cells, respectively; thus, any signal is derived from somatic cells of the testis. The RNAs were subjected to Northern blot analysis using a full-length *Bclw* cDNA probe. To determine whether equal amounts of total RNA had been loaded, the gel was stained with ethidium bromide (EtBr), photographed under ultraviolet (UV) light before transfer, and the blots hybridized with an actin cDNA (lower and middle panels, respectively). A, Testes from adult mouse; RB, residual bodies; RS, round spermatids; at/+, testis from heterozygote atrichosis mouse; at/at, testis from homozygote atrichosis mouse; X/Y, testis from wild-type mouse; XX Sxr, testis from sex-reversed mouse; 7, 12, 17, 22, and 27, testes from Postnatal Day 7, 12, 17, 22, and 27 mice. **B**) Western blot analysis of total protein in preparations of enriched germ cells. Cell preparations enriched for round spermatids (RS) or residual bodies (RB) from adult animals were solubilized, and total protein was analyzed by Western blot analysis using affinity-purified rabbit antisera against a peptide sequence from mouse Bclw [5]. The positive and negative controls include extracts of COS cells transfected with either a mammalian expression vector with a mouse *Bclw* cDNA insert (COS + Bclw) or the same vector without a cDNA insert (COS). Arrowheads indicate the position of the Bclw-specific band. Note the absence of Bclw protein in both RS and RB. **C**) To determine whether equal amounts of protein had been loaded, the blot shown in **B** was stained with Ponceau S before reacting with antisera. Arrowheads denote the approximate size of Bclw (22 kDa). c, COS cells; cb, COS cells transfected with vector expressing Bclw; m, molecular weight markers; rb, enriched for residual bodies; rs, enriched for round spermatids.

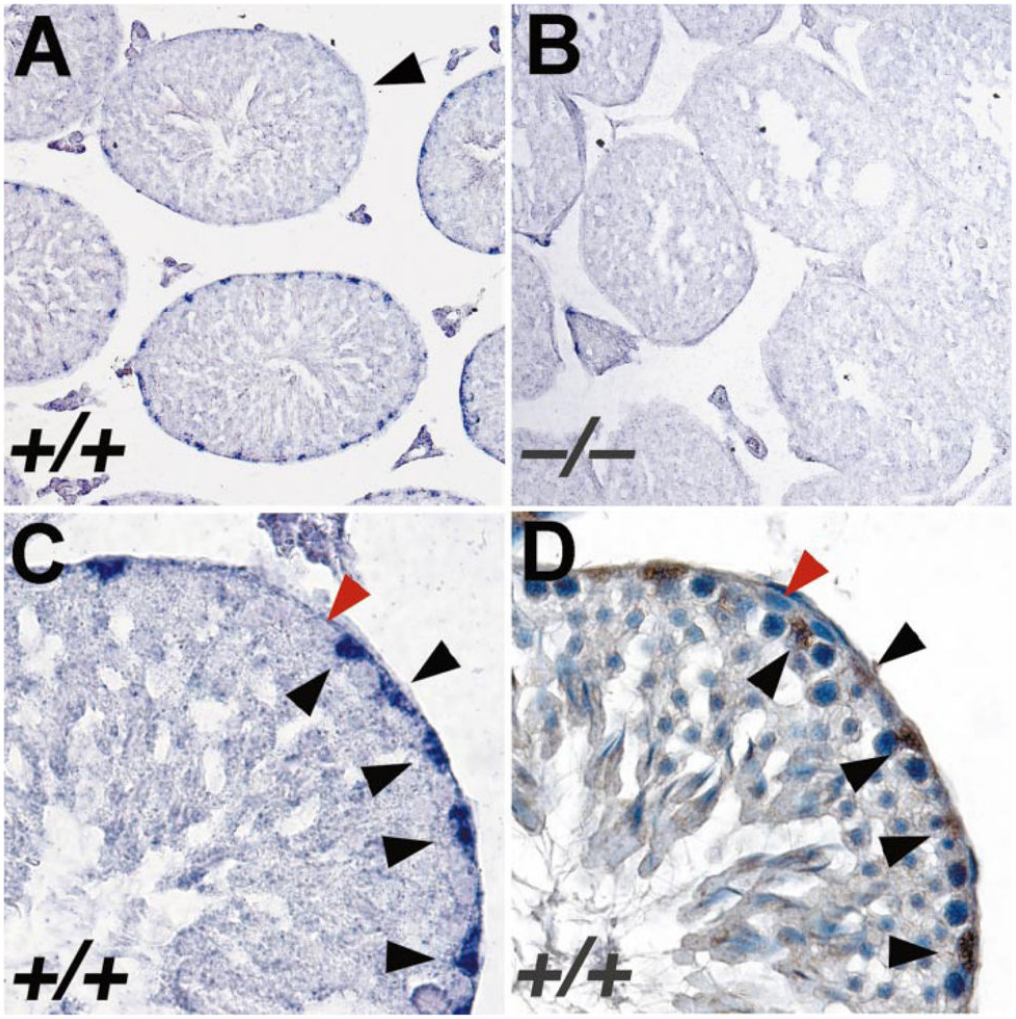

FIG. 2.

In situ hybridization analysis of expression of *Bclw* mRNA in mouse testis. **A**) Section of testis from adult wild-type mouse hybridized with an antisense ribo-probe derived from the 3′-UTR of Bclw cDNA. A significant positive signal (a purple precipitate) is observed only over nuclei of Sertoli cells. Significant signal was observed in all stages of tubules, except those between stages VII and VIII of the seminiferous cycle (arrowhead). ×200. **B**) Section of testis from adult *Bclw* homozygous mutant prepared and analyzed simultaneously under identical conditions as those in **A**. Only background purple precipitate is seen. ×200. **C**) Higher magnification of a single seminiferous tubule from a wild-type mouse, hybridized with anti-sense *Bclw* 3′-UTR riboprobe. Sertoli cell nuclei (black arrowheads) stain relatively intensely purple. In contrast, a spermatogonium (red arrowhead) does not display any significant staining over background. ×640. **D**) Serial section from that shown in **C** reacted with antibody for GATA-1, a marker of Sertoli cell nuclei. The brown staining denotes presence of the antibody. The blue counterstain is hematoxylin. Black and red arrowheads denote the same cells as identified in **C**. ×640.

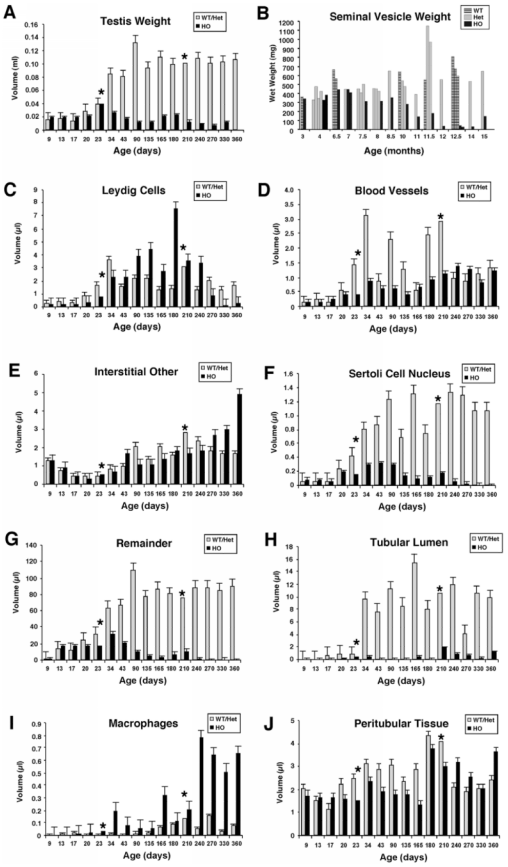

FIG. 3.

Quantitative and morphometric analysis of testicular composition in *Bclw* mutant and control mice. Except for **B**, in each graph the wild-type (WT) and heterozygous mutant (Het) animals are pooled, because no significant difference was found in testicular morphology between these two genotypes. No significant difference was found in weights of seminal vesicles between WT and Het animals, but the values in **B** are presented separately, with each value representing an individual animal. For the remaining graphs, an asterisk indicates that only two animals were in these groups, hence the omission of a bar denoting SEM.

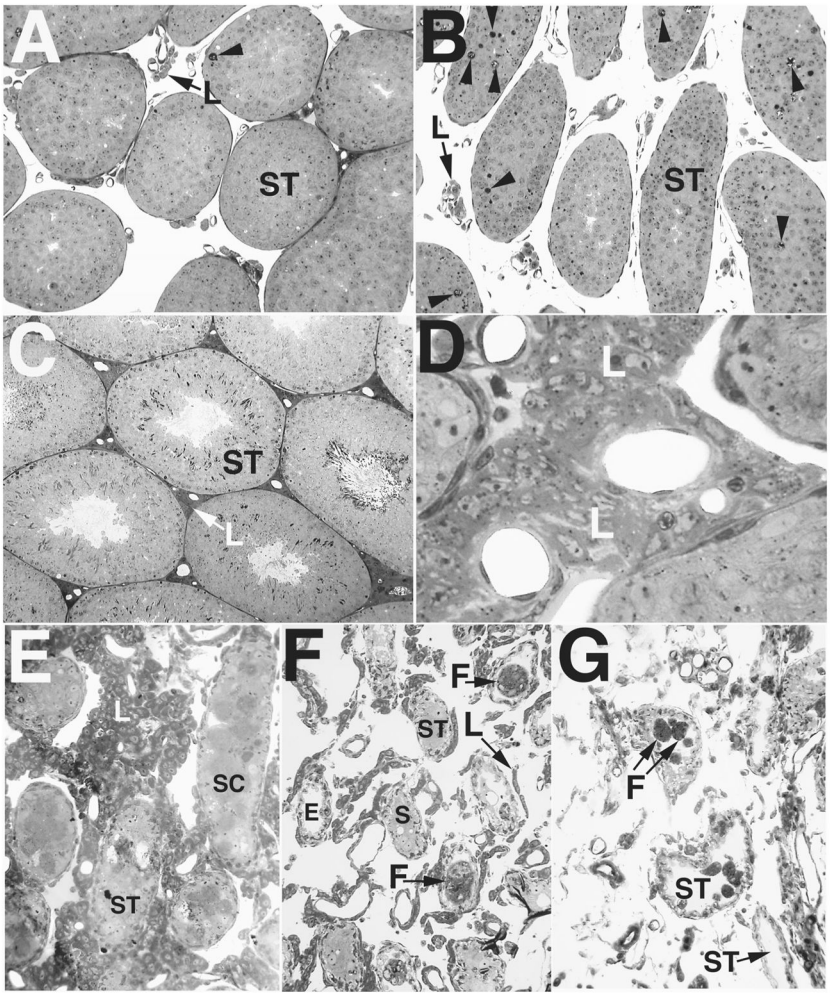

FIG. 4.

Light micrographs showing development of the mutant testicular phenotype in Bclw-deficient mice, emphasizing the general appearance of the testis and the Leydig cells. **A** and **B**) Testes at 20 days of age showing the similar appearance of control (**A**) and *Bclw*-mutant animals (**B**) with respect to Leydig cells (L). As previously described [5], approximately sevenfold more degenerating cells (arrowheads) are seen in the seminiferous tubules (ST) from mutants than in the control. ×70 and ×60, respectively. **C** and **D**) Testes from 3-mo-old animals showing development of the Leydig cells (L) in control (C) and *Bclw*-mutant animals (D). Intertubular clusters of Leydig cells are extensive in *Bclw* mutants. ×80 and ×350, respectively. **E**) Testes from 5.5-mo-old mutants showing the prominent presence of Leydig cells (L). Large masses in seminiferous tubules (ST) were composed of sloughed dead and or dying Sertoli cells (SC). ×155. **F**) Testes from 8-mo-old mutants showing small "strings" of Leydig cells (L) among extremely small seminiferous tubules (ST), with the latter containing some Sertoli cells (S) or foreign-body giant cells (F). A seminiferous tubules devoid of cellular contents (peritubular "ghosts") is marked (E). ×75. **G**) Testes from 12-mo-old mutants with absence of Leydig cells. The scattered cells between peritubular "ghosts" are connective tissue elements and phagocytic elements. A few foreign-body giant cells (F) are seen within seminiferous tubules (ST). ×100.

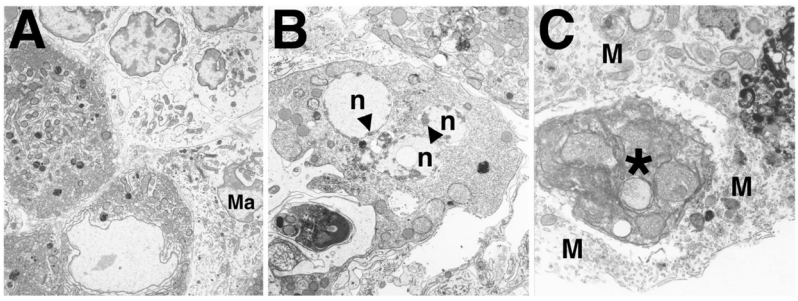

FIG. 5.

Ultrastructural appearance of Leydig cells in *Bclw*-mutants. **A**) At 34 days of age, Leydig cells (darker cells in the lower left) appeared normal. Often, a mononuclear infiltrate was seen in the interstitium (lighter cells in the upper right). A macrophage is also indicated (Ma). ×4500. **B**) Beginning around 8 mo of age, Leydig cells in mutants were observed undergoing apoptosis, as evidenced by the fragmented nuclei (n) and accumulation of associated peripheral heterochromatin (arrowheads). The Leydig cell could be recognized as such by the abundant smooth endoplasmic reticulum and mitochondria possessing tubular cristae and by comparison with relatively normal-appearing, adjacent Leydig cells (top right). ×7200. **C**) Phagocytosis of degenerating Leydig cell (asterisk) by an interstitial macrophage (M). The phagocytosed cell appears dense and contains mitochondria characteristic of those found in Leydig cells. ×14 000.

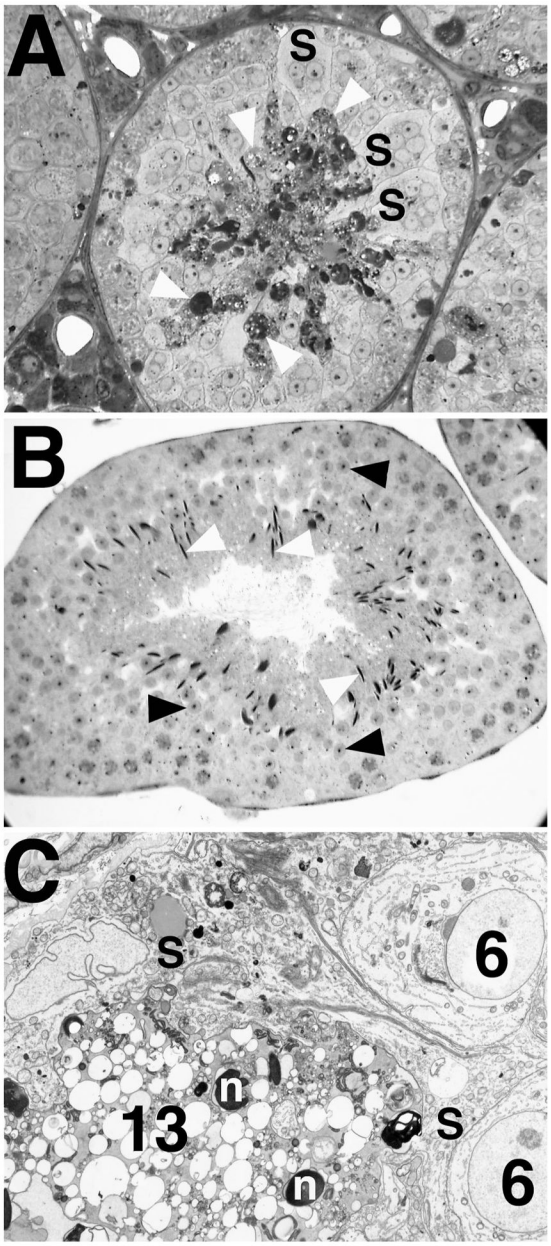

FIG. 6.

Degeneration of elongate spermatids in Bclw-deficient mice. **A**) Light micrograph showing degeneration of step 13 spermatids (white arrowheads), appearing as very dense material, in seminiferous tubules from a *Bclw* homozygous mutant. Symplasts of round spermatids (S) were also commonly seen in mutants. ×275. **B**) Light micrograph showing a comparable stage I tubule in a control animal. Normally developing round (black arrowheads) and elongate (white arrowheads) spermatids are marked. ×170. **C**) Electron micrograph of a stage VI seminiferous tubule from a Bclw-deficient animal. Step 6 (6) spermatids are associated with a dense, degenerating symplast of step 13 (13) spermatids (lower left) that is contained in a single, dense cytoplasmic mass in contact with Sertoli cells (S). Step 13 spermatid nuclei (n) are indicated. ×3200.

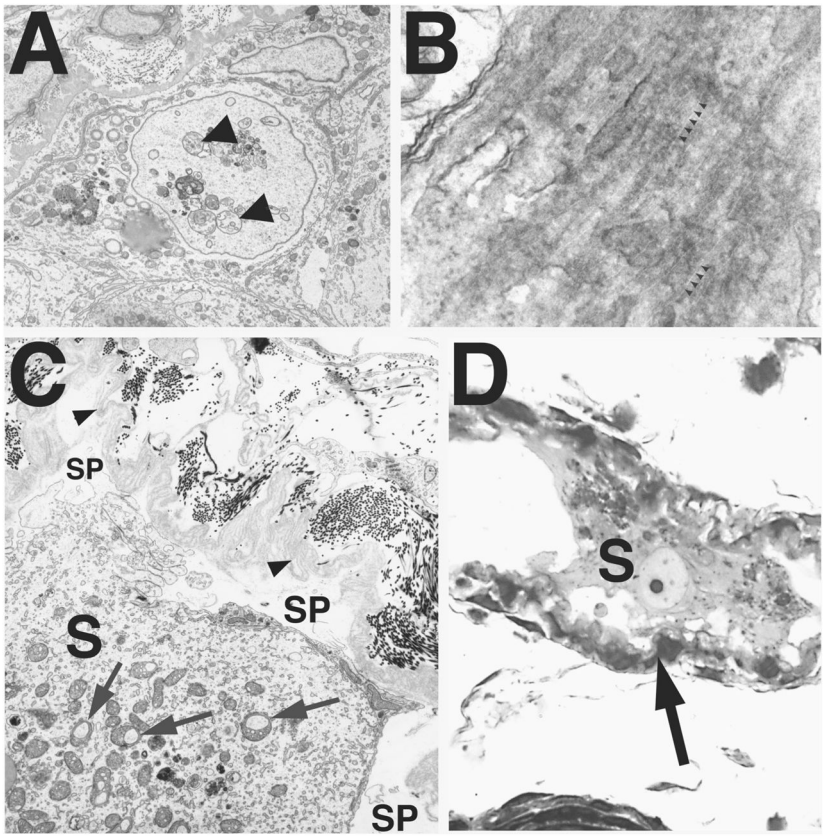

FIG. 7.

Morphological features of Sertoli cells in Bclw-deficient animals. **A**) Nuclear vacuolation (arrowheads) within the nucleus of a Sertoli cell located centrally within the micrograph. Many mitochondria appear swollen. ×3300. **B**) *En face* section of Sertoli-Sertoli junctions in p90 Bclw-deficient animal showing both actin filament bundles (gray parallel amorphous material running from lower left to upper right) and translucent linearities (small black arrowheads) in the areas of occluding junction representing fusions of membranes. ×85 000. **C**) Loss of attachment of Sertoli cells from the seminiferous tubule and from each other in a *Bclw*-mutant more than 6 mo of age. Spaces where the Sertoli cell (S) has not maintained contact with the highly infolded and duplicated basal lamina (arrowheads) are indicated (SP). No other Sertoli cell was seen at the lateral borders of this Sertoli cell (not shown). Many mitochondria in the Sertoli cytoplasm appear swollen (arrows). ×10 000. **D**) Light micrograph of a single Sertoli cell (S) in a greatly shrunken tubule from a *Bclw* mutant more than 6 mo of age containing only peritubular cells of the tunica propria (arrow). No other Sertoli cell was seen at its lateral borders. Note the vacuolation within the Sertoli cell cytoplasm. No Leydig cells are shown. ×1200.

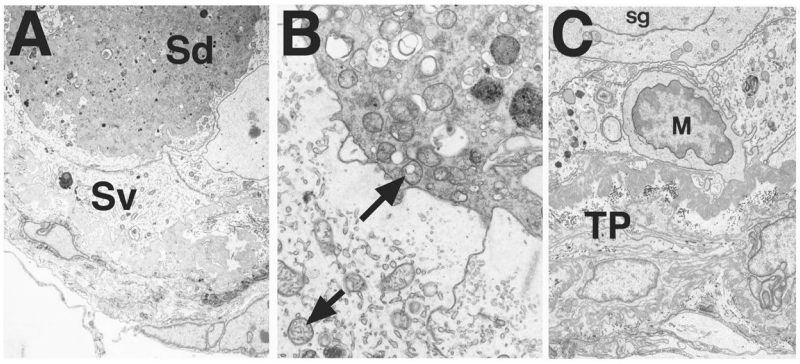

FIG. 8.

Electron micrographs illustrating degenerating Sertoli cell masses located centrally within seminiferous tubules in 9-mo-old *Bclw* mutants. **A**) A large, dense Sertoli cell mass (Sd) is located in the center of a germ cell-depleted tubule adjacent to a viable Sertoli cell (Sv). ×4000. **B**) The interface of a highly densified, dying or dead Sertoli cells (upper right) with normal-appearing, viable Sertoli cells (lower left) shows the mitochondria of both to be characteristic, mouse-type Sertoli cell mitochondria (arrows). ×18 000. **C**) Inactivated macrophage (M) within the seminiferous tubule among Sertoli cells and a spermatogonium (sg). The tunica propria (TP) of the tubule is at the bottom of the figure. ×5500.

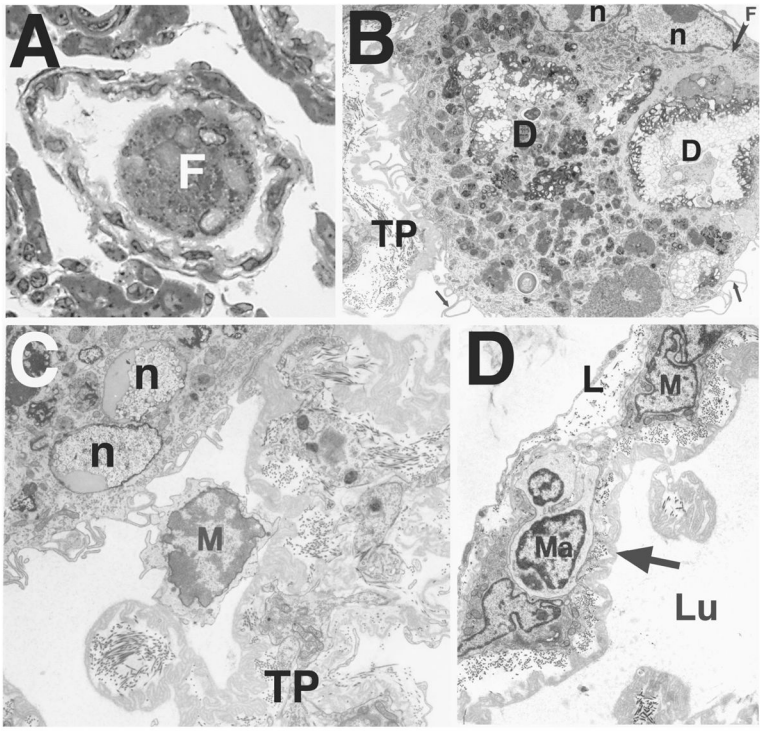

FIG. 9.

Formation of foreign-body giant cells in seminiferous epithelium of *Bclw*-mutants. **A**) Light micrograph showing a foreign-body giant cell (F) in the seminiferous tubules of a Bclw-deficient mouse. ×1100. **B**) Electron micrograph of a foreign-body giant cell. These extremely large, phagocytic foreign-body giant cells (arrow, F) contain phagocytosed material and were seen primarily in tubules depleted of cells, with only the peritubular cells of the tunica propria (TP) at the left remaining. Ultrastructurally, foreign-body giant cells display multiple nuclei (n), microvillous processes (small arrows at bottom), and an abundance of semidigested cellular remnants (D) contained within residual bodies. ×5000. **C**) Seminiferous tubule with only a tunica propria (TP) lining and intratubular macrophages (M). Both an inactivated macrophage (M) and a portion of a foreign-body giant cell showing multiple nuclei (n) are seen. ×5000. **D**) Electron micrograph of the peritubular cell tunica propria forming the wall of a seminiferous tubule lacking cellular contents. Identified are the tubular lumen (Lu), the myoid cell (M), a thin and lymphatic endothelial cell (L), and the infolded and duplicated basal lamina (arrow) lying internal to the myoid cell. Also identified is a macrophage (Ma) within the tunica propria. ×6000.